

Miniature Broadband Bandpass Filters Using Double-Layer Coupled Stripline Resonators

Yunchi Zhang, *Student Member, IEEE*, Kawthar A. Zaki, *Fellow, IEEE*, Andrew J. Piloto, and Joseph Tallo

Abstract—A novel double-layer coupled stripline resonator structure is introduced to realize miniature broadband bandpass filters. Filters with relative bandwidth up to 60% and size less than $\lambda/8 \times \lambda/8 \times h$ (λ is wavelength at the midband frequency; h is the substrate height, which is much smaller than $\lambda/8$) can be fulfilled using such resonators. Two possible filter configurations are proposed in this paper: combline and interdigital. The filter synthesis procedure follows the classical coupling matrix approach that generates very good initial responses. Optimization by the mode-matching method and fine tuning in Ansoft's High Frequency Structure Simulator are combined to improve the filter performance. Two filter design examples are given to validate the feasibility. Low temperature co-fired ceramic (LTCC) technology is employed to manufacture the filters. Experimental results of the two manufactured filters are presented. The effects of LTCC manufacturing procedure on the filter performance are also discussed.

Index Terms—Bandpass filter, broadband, combline, compact, interdigital, low-temperature co-fired ceramic (LTCC), miniature, resonator, stripline.

I. INTRODUCTION

MINIATURE broadband filters compatible with printed circuit board (PCB) and monolithic-microwave integrated-circuit (MMIC) fabrication technologies are required in many communication systems. The filter size is usually constrained by the size of the employed resonator structures, and the filter bandwidth is limited by the achievable maximum couplings between these resonators. Many available compact resonator structures can be found in literatures. Some of them, such as a stripline resonator with one grounded end [1], hairpin resonator [2], etc., have the size constraint of a quarter-wavelength. Others, such as folded quarter-wavelength resonator [3], ring resonator [4], spiral resonator [5], etc., have a smaller size than a quarter-wavelength, but are usually not applicable for broadband filter designs due to the difficulty in realizing the strong couplings.

The goal of this paper is to design broadband filters with compact size less than $\lambda/8 \times \lambda/8 \times h$ (filter height h is usually very small and approximately equal to the substrate height of the stripline). A novel double-layer coupled stripline resonator structure is, therefore, proposed to fulfill the purpose. The size of the proposed resonator structure can be less than $\lambda/12$, and the coupling between two resonators can be realized strong enough

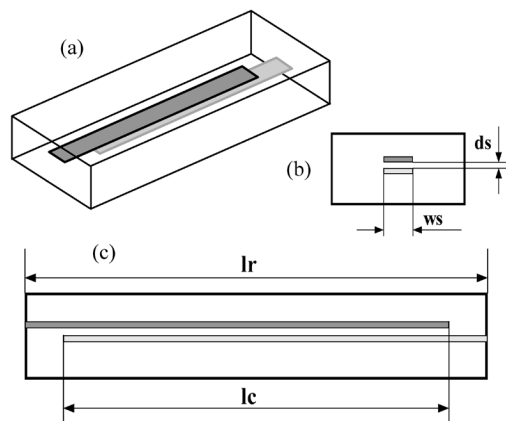


Fig. 1. Double-layer coupled stripline resonator structure. (a) Three-dimensional view. (b) Cross section. (c) Side view. The structure is filled with a homogeneous dielectric material.

for filter designs up to 60% bandwidth by proper mechanisms. Physical realization of the resonator structure can be easily performed in low-temperature co-fired ceramic (LTCC) technology that is a suitable manufacturing choice for a high-integration level of multiple-layer structures.

Two types of filter configurations can be implemented using the proposed resonator structures: combline and interdigital [6]. In this paper, two design examples of interdigital filters are presented to validate the theory. The two filters having the same specifications, but employing different resonator dimensions are manufactured to investigate the LTCC manufacturing effects on the performance.

II. FILTER CONFIGURATION

A. Proposed Resonator Structure

The proposed double-layer coupled stripline resonator structure is shown in Fig. 1. The idea is to introduce a strong capacitive loading effect inside the resonator to reduce its physical length [7]. The resonator structure consists of two strongly coupled strips, as shown in Fig. 1(b). The opposite ends of these two strips are shorted to ground, as shown in Fig. 1(c), so the coupling between these two strips will behave like a capacitance that will lower the resonant frequency. Due to this capacitive coupling effect, the total physical length lr of the resonator will be much shorter than a quarter-wavelength at the desired resonant frequency. The physical length lr of the resonator is determined by three factors, which are: 1) the width ws of the two strips; 2) the coupled (overlapped) length lc ; and 3) the vertical distance ds between them because these three factors will affect the capacitive coupling between the two strips. Actually,

Manuscript received April 6, 2006; revised May 15, 2006.

Y. Zhang and K. A. Zaki are with the Department of Electrical and Computer Engineering, University of Maryland at College Park, College Park, MD 20742 USA (e-mail: ychzhang@umd.edu).

A. J. Piloto and J. Tallo are with Kyocera America, San Diego, CA 92123 USA (e-mail: Andy.Piloto@kyocera.com).

Digital Object Identifier 10.1109/TMTT.2006.879176

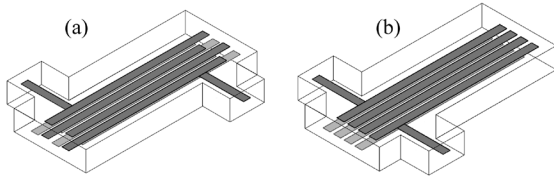


Fig. 2. Proposed filter configurations using double-layer coupled stripline resonators. (a) Interdigital filter configuration. (b) Comblines filter configuration.

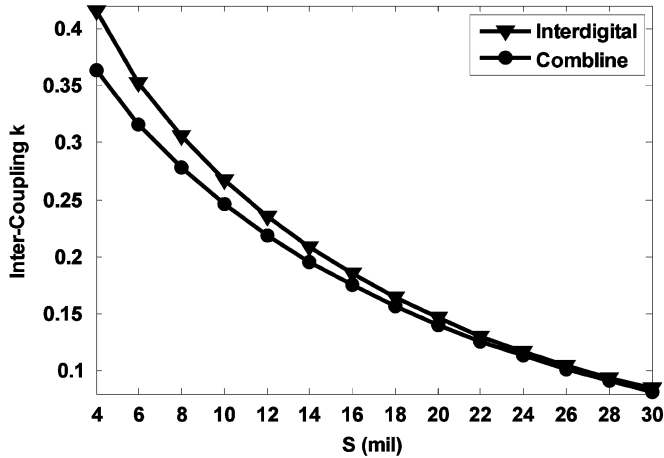


Fig. 3. Inter-coupling curves of interdigital and comblines configurations. Identical resonators are used. S is the separation between two resonators.

resonator with physical length less than $\lambda/12$ at the desired resonant frequency can be realized by such a configuration with properly selected dimensions of these three factors.

It must be noted that the vertical distance ds between the two strips must be an integer multiple of the thickness of one ceramic layer in LTCC technology, and so is the whole height of the resonator.

B. Possible Filter Configurations

Shown in Fig. 2 are two possible filter configurations using the proposed double-layer coupled stripline resonators: interdigital as in Fig. 2(a), and comblines as in Fig. 2(b). These two filter structures are more compact compared with conventional one-layer microstrip/stripline interdigital and comblines filters. The input/output external couplings are realized by the tapped-in $50\text{-}\Omega$ striplines. The inter-coupling between resonators is achieved by the fringing fields between two resonator lines. Usually the coupling between two interdigital resonators is stronger than the coupling between two comblines resonators having the same spacing [8]. Shown in Fig. 3 are the coupling curves for both cases with identical resonator dimensions. The smaller the separation between two resonators, the more noticeable the coupling difference between the two configurations. Therefore, interdigital configuration is more appropriate for broadband filter designs, while comblines configuration is a proper choice for some relatively narrower bandwidth filter designs since it has more compact size than the interdigital one.

III. FILTER DESIGN AND MODELING

To design a filter with either of the proposed configurations in Fig. 2, the following three steps are implemented.

- Step 1) Initial filter dimensions are determined according to the given filter specifications.
- Step 2) Optimization using the mode-matching method (MMM) is performed to find the optimum filter dimensions.
- Step 3) Ansoft's High Frequency Structure Simulator (HFSS) is employed to check the optimum design from (2) and fine tune the filter dimensions if needed.

The detailed information is illustrated below.

A. Initial Design

Given the specifications of a desired filter, the filter design starts with synthesizing a circuit model prototype. Physical realization is then performed according to such ideal model. For the cases presented in this paper, the initial design procedure is given as follows.

- 1) An ideal circuit model is generated according to the filter requirements [9].
- 2) The dimensions of the double-layer coupled stripline resonator are determined in terms of the center frequency of the filter.
- 3) Determine the tapped-in stripline position to achieve the external coupling R [6], [10].
- 4) Determine the separations between resonators to provide the required inter-couplings [6], [11].
- 5) Assemble the tapped lines and resonators together according to the calculated dimensions. Initial filter responses can be obtained by full-wave electromagnetic simulation in MMM or Ansoft's HFSS.

One of the advantages of comblines and interdigital filters is that the resonant frequency of the resonators will not be changed much by the loading effects of the couplings. Therefore, the initial filter response is usually a good starting point (return loss is typically below 10 dB) for further optimization.

B. Optimization by MMM

The initial design procedure given above does not take into account the higher order modes and the nonadjacent couplings between resonators, which have more effects on broadband filter designs than narrowband ones. To achieve the desired filter performance, optimization by MMM can be employed. To demonstrate the optimization procedure by MMM, an interdigital filter configuration is used (the comblines case is similar).

Shown in Fig. 4(a) is an interdigital filter with two stripline ports along the z -axis. To model this filter configuration, the MMM should be applied along the z -direction. The cross sections involved are a stripline (I), an asymmetric stripline (II), side view of a double-layer coupled stripline resonator (III), a rectangular waveguide (IV), etc. [as in Fig. 4(b)]. Eigenmodes and eigenfields of these cross sections can be calculated as in [12] and [13]. Basically, a given cross section is decomposed into many parallel-plate regions and the eigenfields in each region are expressed as a summation of Fourier series with unknown coefficients. By applying the boundary conditions

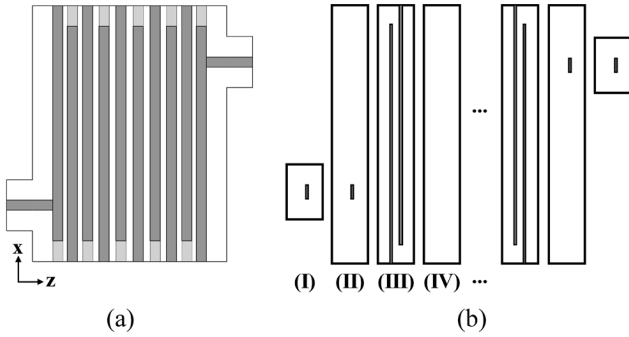


Fig. 4. (a) Tenth-order interdigital filter using double-layer coupled stripline resonators. (b) Involved cross sections along z -axis.

and the field-continuity conditions between the parallel-plate regions, a linear system is obtained and the solution of this system will lead to the cutoff frequencies of eigenmodes and the coefficients of Fourier series. Accordingly, the eigenfields of the total cross section can be solved. The discontinuities between these cross sections are modeled by generalized scattering matrices (GSMs) solved according to the matching boundary conditions [13]. Finally, the overall response can be calculated by cascading all the GSMs together.

In principle, this MMM approach is very rigorous, but the convergence and simulation speed must be considered. The rectangular waveguides separating the discontinuities are very short, and the fundamental resonating modes of the interdigital filter are mainly operating with TEM^x fields, while the fields in cross sections of III, IV, etc. are presented as a summation of TE^z and TM^z modes in the MMM analysis. As a consequence, a very large number of modes are needed for convergence, which would result in large computation time and numerical errors. In order to do the optimization with this MMM approach, the appropriate number of modes should be selected to have the fast optimization speed and acceptable simulation results. Usually the simulation durations and responses using different number of modes are examined, and a tradeoff between simulation speed and accuracy is made to select the number of modes for optimization.

The tapped-line position, widths of resonators, and separations between resonators can be optimized to improve the filter performance. The error function to be minimized is constructed depending on the locations of the poles (f_{pi}) and equal-ripple points (f_{ei})

$$\text{err} = \sum_{i=1}^{N_p} w_{pi} |s_{11}(f_{pi})|^2 + \sum_{i=1}^{N_e} w_{ei} (|s_{11}(f_{ei})| - \varepsilon)^2 \quad (1)$$

where N_p and N_e are the number of poles and equal-ripple points, respectively. w_p and w_e are the optimization weights. ε represents the equal-ripple return loss.

C. Fine-Tuning in HFSS (If Needed)

The optimized filter response by the MMM with the selected number of modes might be different from the converged one. Ansoft's HFSS is then applied to verify the design and fine tune the filter if needed. The parameter extraction method [14] can be employed to guide the fine tuning in HFSS to speed up the

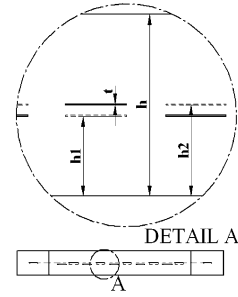


Fig. 5. End view along x -direction of the filter configuration in Fig. 4(a).

procedure. Basically, only the tapped-line position and the width of the first resonator are needed to be tuned in this step.

HFSS is not used in the previous optimization step because of the slow simulation speed. For the design examples in this paper, it takes MMM approximately 5 h and 1000 iterations to generate the desired performance after the eigenmodes and eigenfields have been calculated (150 modes are used), while it takes HFSS more than 6 h to obtain the converged response for one single filter structure. For an optimization procedure of 1000 iterations, it will take HFSS approximately 6000 h to acquire the optimum design, which is not acceptable. A desktop PC using 3.0-GHz Pentium 4 processor and 4-GB memory is employed to perform the designs.

IV. DESIGN EXAMPLES

Two design examples of interdigital filters are performed to show the feasibility. They have the same specifications, but different resonator dimensions, and are manufactured to investigate the effects of the LTCC manufacturing procedure.

A. Design Example 1

A design of a ten-pole Chebyshev filter with a center frequency of 1.125 GHz and 500-MHz bandwidth is performed. The relative bandwidth is approximately 45%. The desired stop-band rejection level below 0.75 GHz and above 1.5 GHz must be larger than 50 dB. The external couplings and the normalized inter-couplings are

$$\begin{aligned} R_{in} &= R_{out} = 0.98562 \\ m_{12} &= 0.81907 \\ m_{23} &= 0.58576 \\ m_{34} &= 0.54538 \\ m_{45} &= 0.53288 \\ m_{56} &= 0.52976. \end{aligned} \quad (2)$$

The interdigital filter configuration to be employed is shown in Fig. 4(a). This filter will be embedded inside a PCB system using LTCC technology, and the stack-up options with other components set many constraints on the vertical dimensions. Shown in Fig. 5 is the end view of the filter along the x -direction. The height of the whole filter box is $h = 59.28$ mil, the vertical position of the lower strip is $h_1 = 25.94$ mil, and the vertical position of the upper strip is $h_2 = 29.69$ mil. Only one ceramic layer (thickness is approximately 3.74 mil) exists between the two strips. The metallization thickness of the strip is $t = 0.4$ mil

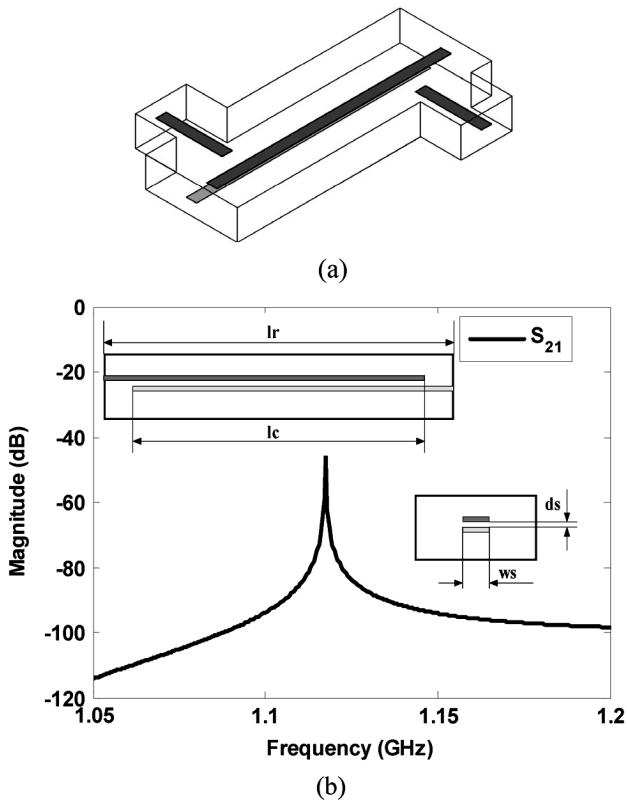


Fig. 6. (a) Configuration to decide the dimensions of the resonator. (b) Typical frequency response of S_{21} for configuration (a).

and the relative permittivity of the ceramic is $\epsilon_r = 5.9$, which are decided by the selected LTCC technology.

Fig. 6(a) is the configuration to determine the resonator dimensions to have the fundamental resonating mode at the center frequency of 1.125 GHz. Two ports are weakly coupled to the resonator and the peak frequency of the simulated S_{21} response, as shown in Fig. 6(b), is the resonant frequency. The length lr of the resonator is selected as $lr = 500$ mil. The coupled length lc and width ws of the two strips (two strips in one resonator have the same dimensions) are being swept until the required resonant frequency of 1.125 GHz is achieved. The found values are $lc = 420$ mil and $ws = 20$ mil.

The external coupling curve is presented in Fig. 7, which shows the external coupling is linearly proportional to the tapped-in position. The value of $htapin$ to have $R = 0.98562$ is approximately 432 mil.

The computed inter-coupling curve is shown in Fig. 8 and the separations are calculated by interpolation to have the desired inter-couplings. The found separations for the five desired adjacent couplings in (2) are $S_{12} = 7.1$ mil, $S_{23} = 11.9$ mil, $S_{34} = 13.0$ mil, $S_{45} = 13.4$ mil, and $S_{56} = 13.5$ mil, respectively.

The initial filter response is presented in Fig. 9. The simulated frequency responses by MMM and HFSS of the final filter design are both shown in Fig. 10, which demonstrates a good agreement between them.

The minimum return loss over the passband is approximately 15 dB because the nonadjacent couplings for such broadband filter are not avoidable and make it very difficult

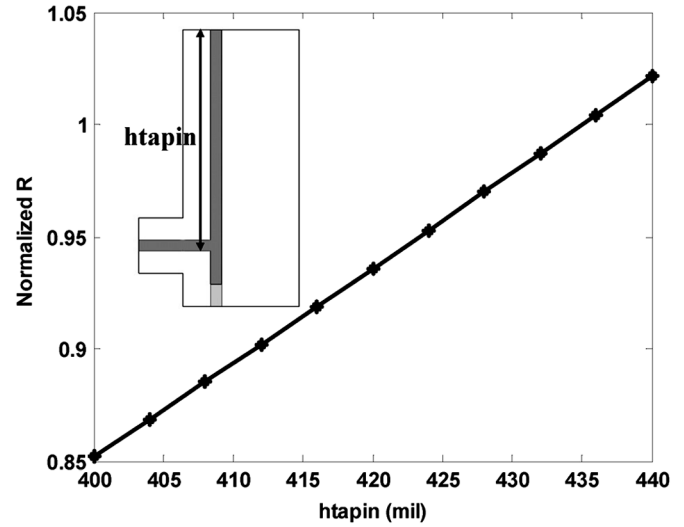


Fig. 7. External coupling curve: normalized R versus tapped-in position $htapin$.

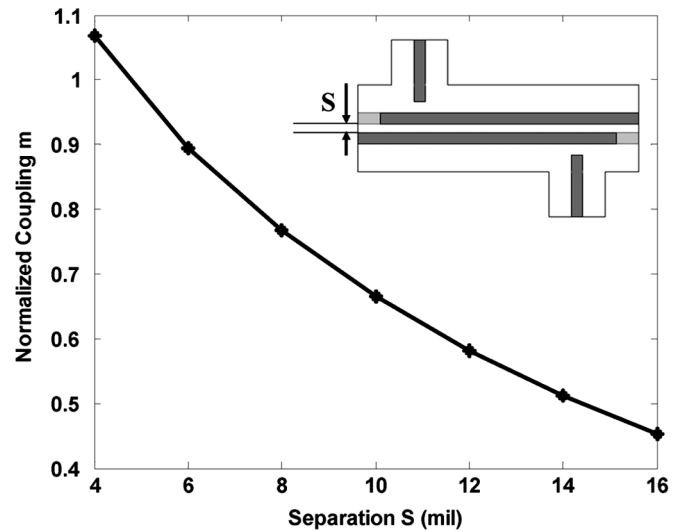


Fig. 8. Inter-coupling curve: normalized coupling m versus separation S .

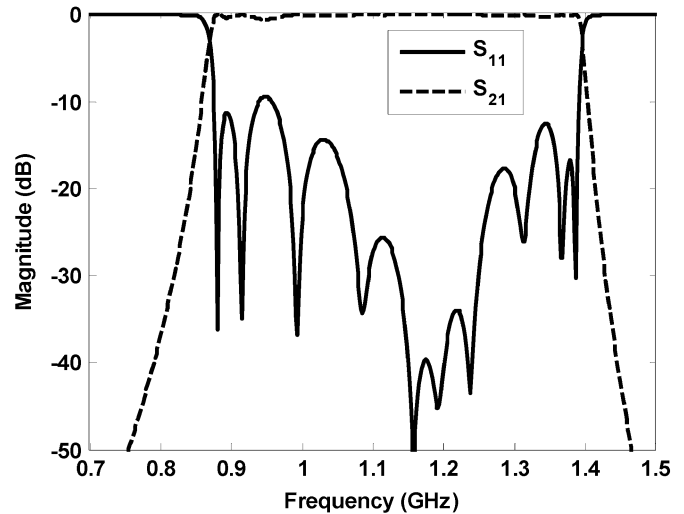


Fig. 9. Frequency response of filter example I with initial dimensions.

to achieve a return loss better than 15 dB. The upper stopband of this filter has clean spurious response up to the third

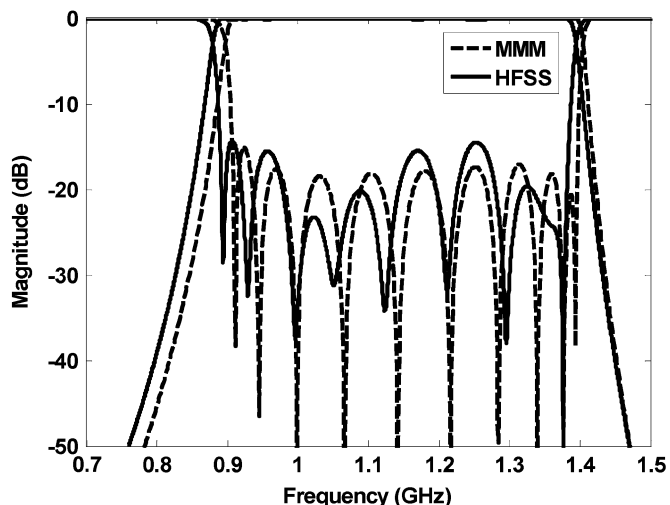


Fig. 10. Simulated responses of the optimized filter I by MMM and HFSS.

harmonic. The final dimension of the whole filter box is approximately $500 \text{ mil} \times 515 \text{ mil} \times 59.28 \text{ mil}$, which is less than $\lambda/8 \times \lambda/8 \times h = 540 \text{ mil} \times 540 \text{ mil} \times 59.28 \text{ mil}$ at the center frequency of 1.125 GHz.

This filter is manufactured in LTCC technology for testing. Fig. 11(a) shows the filter prototype and the arrangement of the measurement. Input and output ports of the filter are bent toward the same direction for the convenience to connect with other components. Transitions from $50\text{-}\Omega$ microstrip lines to the tapped-in striplines are also added on the filter. J -probe launches and a Cascade Microwave Probe Station are used in the measurement. The measured response is shown in Fig. 11(b). The insertion loss at the center frequency is approximately 3 dB and at the higher band edge is approximately 6 dB. The wideband response shows that the spurious response that starts around 3.6 GHz is approximately three harmonics. A simulation by HFSS with lossy materials is also performed to investigate the response difference between the designed and manufactured filters. The employed parameters for loss are: finite conductivity $\sigma = 13100000 \text{ S/m}$ for conductor and loss tangent of 0.001 for ceramics. Both the simulated and measured responses are shown in Fig. 11(c). A good agreement is noticed, except a frequency shift between them. The frequency shift is caused by the effects of the LTCC manufacturing procedure such as vias, inhomogeneous ceramic layers, etc. (in HFSS simulation, solid walls and homogeneous materials are assumed), which will be discussed later.

B. Design Example II

In design example I, one ceramic layer of thickness $ds = 3.74 \text{ mil}$ exists between the two strips of a resonator. To investigate the sensitivity of the filter with respect to ds and the effects of the LTCC manufacturing procedure on filter performance, a second design with larger ds is carried out for an odd-order interdigital filter. The filter requirements are identical with design example I, but a design of an eleven-pole filter is performed for this example. The stack-up option is different from example I. For this example, $h_1 = 29.68 \text{ mil}$, $h_2 = 37.08 \text{ mil}$, and $h = 63.02 \text{ mil}$. Definitions of h_1 , h_2 , and

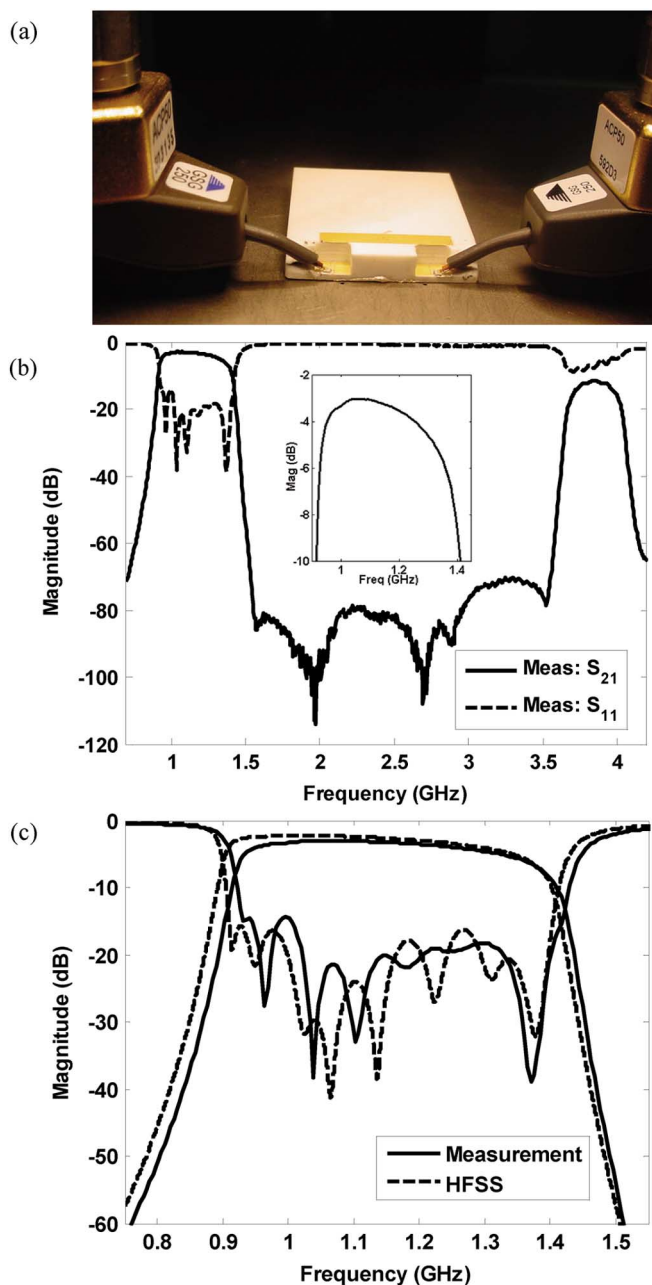


Fig. 11. (a) Built filter I and the measurement arrangement. (b) Measured frequency response of filter I. (c) Comparison between the measurement and simulated response by HFSS. (Color version available online at: <http://ieeexplore.ieee.org>.)

h are given as shown in Fig. 5. The separation between the two strips is $ds = h_2 - h_1 = 7.4 \text{ mil}$, which means that the physical length of the resonator will be longer than example I due to the relatively weaker coupling between two strips. The selected dimensions of the resonator are $lr = 700 \text{ mil}$, $lc = 516 \text{ mil}$, and $ws = 20 \text{ mil}$.

The same design procedure as example I is followed for this design. The final dimension of the whole filter box is approximately $700 \text{ mil} \times 540 \text{ mil} \times 63.02 \text{ mil}$, which is larger than design example I. Fig. 12 shows both manufactured filters of examples I and II. The measured response is shown in Fig. 13(a). The spurious response starts around 2.5 GHz, which is about

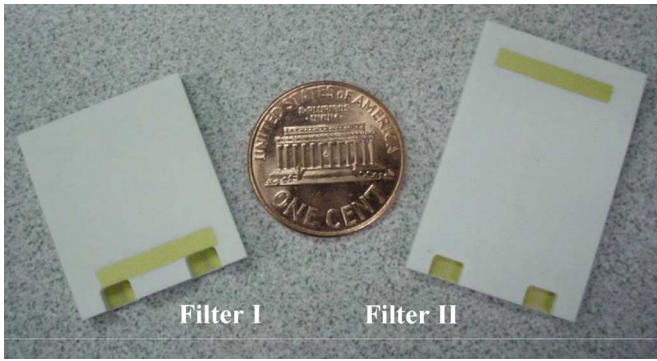


Fig. 12. Manufactured filters (design example I and design example II). Filter II is slightly larger than filter I. (Color version available online at: <http://ieeexplore.ieee.org>.)

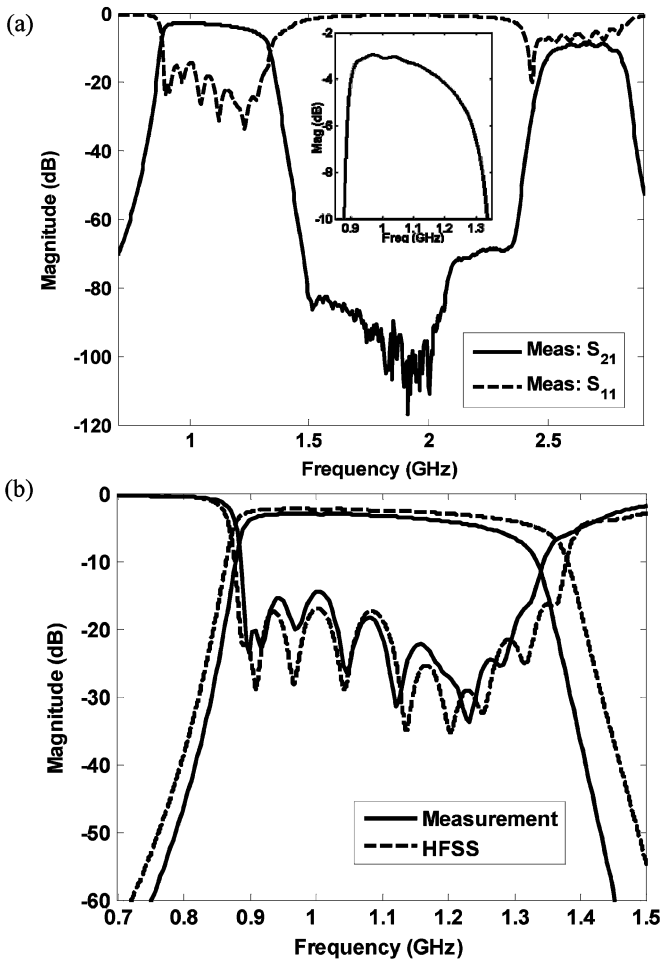


Fig. 13. (a) Measured response of filter II. (b) Comparison between the measurement and the simulated response by HFSS.

two harmonics. The reason why filter II has worse spurious performance than filter I is related to the resonator structure and dimensions. The first higher order resonating mode of the resonator is controlled by the introduced capacitive coupling between two strips. The stronger the coupling, the further the first higher order mode. Resonators in filter II has larger ds than filter I and, thus, smaller capacitive coupling between strips; therefore, the first higher order resonating mode is closer to the center

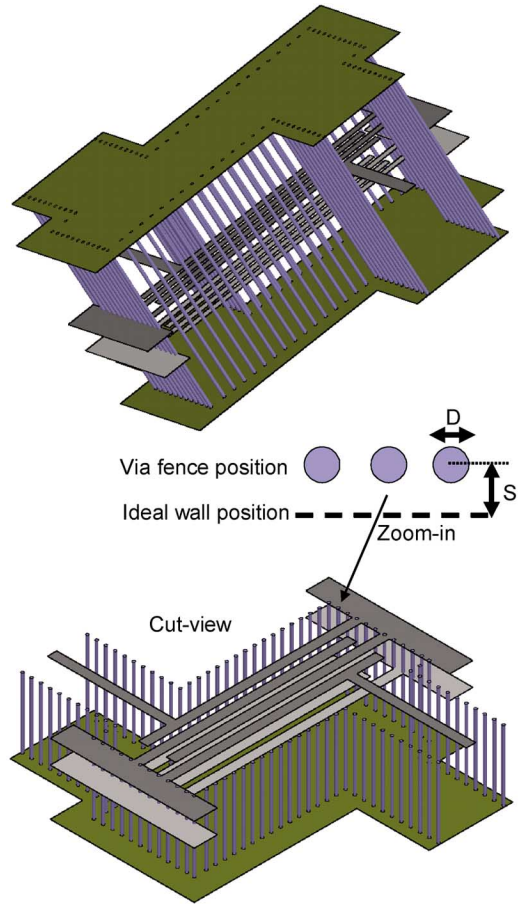


Fig. 14. Draft of the physical realization of filters in LTCC technology. (Color version available online at: <http://ieeexplore.ieee.org>.)

frequency, which causes the spurious performance to be worse than filter I. The response comparison between the measurement and HFSS simulation is shown in Fig. 13(b). The measured bandwidth is slightly narrower than the simulated one, which is also due to the manufacturing effects.

In both design examples, the measured insertion loss is slightly larger than the simulated one. Two main reasons are responsible for that, which are: 1) vias in actual structures might introduce more loss than the solid wall model in HFSS and 2) the loss tangent of the actual ceramic material is larger than 0.001.

V. LTCC MANUFACTURING EFFECTS ON FILTER PERFORMANCE

The measured responses of the two filters are slightly different from the simulated ones, which is usually caused by the LTCC manufacturing effects. Shown in Fig. 14 is a draft of the physical realization of the designed filters in LTCC technology. Basically, the filled ceramic is placed layer by layer with fixed thickness of each layer. The horizontal walls and resonator striplines inside the ceramic are implemented by metallization of gold. The vertical walls are realized by a via-fence of closely placed vias. If the signal is communicating between different layers, vias are also applied to connect the signal lines. Such a manufacturing procedure will affect the filter performance from several points-of-views.

First, the via-fence to realize the vertical walls of the filter will affect the resonator length, which can be observed from the zoom-in view of Fig. 14. Diameter D of vias is approximately 6 mil. The distance between two vias should be selected to be as small as possible to decrease the parasitic resistance and also create an effective "pure resistance" environment (i.e., parasitic inductance and capacitance are counteracted), which is usually decided experimentally. The via-fence position relative to the ideal vertical wall position (S in Fig. 14) should be determined to have the manufactured resonator resonating at the same frequency as the ideal resonator, otherwise the actual filter response will be shifted from the designed one. The optimum via-fence position is approximately $S = D/4$.

Second, the thickness of gold metallization usually varies from 0.4 to 0.6 mil. This effect will cause the variation of the vertical distance ds (as in Fig. 1) between two strips in a resonator and, thus, the frequency shift of the resonators. The filters designed with smaller ds will be influenced more by this effect than those with larger ds since the variation occupies more percentage in smaller ds . This might be one of the reasons that the measured response of filter I is shifted from the desired center frequency.

Third, assembling the filled ceramic layer-by-layer causes the variation of the permittivity of different layers, i.e., the filled ceramic is not perfectly homogeneous. The relative permittivity can be from 4.7 to 6.3. This effect will cause the frequency shift and mainly influence all the couplings existing in the filters. The filters with larger ds will be affected more since larger ds means greater variation of the permittivity. This could be one of the reasons that filter II has narrower bandwidth than the design bandwidth.

In the actual manufacture, several test pieces are usually manufactured and measured first. The proper processing conditions to reduce the aforementioned effects are then determined according to the comparison between the measured response and the designed one. Once the processing conditions are found, the mass production of components can be performed with more than 95% yield.

VI. CONCLUSION

A novel double-layer coupled stripline resonator has been introduced for compact size and broadband bandpass filter designs. Two interdigital filter examples using such resonators have been presented. LTCC technology has been employed to manufacture the filters and the effects of LTCC manufacturing procedure on the filter performance have been discussed. The experimental results are in good agreement with the designed responses, validating the theory and design method.

ACKNOWLEDGMENT

The authors would like to acknowledge Dr. J. A. Ruiz-Cruz, Universidad Autónoma de Madrid, Madrid, Spain, for his helpful discussions.

REFERENCES

[1] G. L. Matthaei, L. Young, and E. M. T. Jones, *Microwave Filters Impedance-Matching Networks and Coupling Structures*. Norwood, MA: Artech House, 1980.

- [2] E. Cristal and S. Frankel, "Hairpin-line and hybrid hairpin-line/half-wave parallel-coupled-line filters," *IEEE Trans. Microw. Theory Tech.*, vol. MTT-20, no. 11, pp. 719–728, Nov. 1972.
- [3] C.-Y. Chang, C.-C. Chen, and H.-J. Huang, "Folded quarter-wave resonator filters with Chebyshev, flat group delay, or quasi-elliptical function response," in *IEEE MTT-S Int. Microw. Symp. Dig.*, Jun. 2–7, 2002, vol. 3, pp. 1609–1612.
- [4] K. Chang, *Microwave Ring Circuits and Antennas*. New York: Wiley, 1996, ch. 3, 7, and 12.
- [5] F. Huang, "Ultra-compact superconducting narrowband filters using single- and twin-spiral resonators," *IEEE Trans. Microw. Theory Tech.*, vol. 51, no. 2, pp. 487–491, Feb. 2003.
- [6] Y. Zhang and K. A. Zaki, "Compact, coupled strip-line broadband bandpass filters," presented at the IEEE MTT-S Int. Microw. Symp., Jun. 2006.
- [7] L. A. Robinson, "Wideband interdigital filters with capacitively loaded striplines," in *IEEE MTT-S Symp. Dig.*, May 1965, vol. 65, pp. 33–38.
- [8] R. Levy, R. V. Snyder, and G. Matthaei, "Design of microwave filters," *IEEE Trans. Microw. Theory Tech.*, vol. 50, no. 3, pp. 783–793, Mar. 2002.
- [9] A. E. Atia, A. E. Williams, and R. W. Newcomb, "Narrow-band multiple-coupled cavity synthesis," *IEEE Trans. Circuits Syst.*, vol. CAS-21, no. 9, pp. 649–655, Sep. 1974.
- [10] M. El Sabbagh, H. T. Hsu, and K. A. Zaki, "Full-wave optimization of stripline tapped-in ridge waveguide bandpass filters," in *IEEE MTT-S Int. Microw. Symp. Dig.*, Jun. 2002, vol. 3, pp. 1805–1808.
- [11] J.-S. Hong and M. J. Lancaster, *Microstrip Filters for RF/Microwave Applications*. New York, NY: Wiley, 2001.
- [12] Y. Rong and K. A. Zaki, "Characteristics of generalized rectangular and circular ridge waveguides," *IEEE Trans. Microw. Theory Tech.*, vol. 48, no. 2, pp. 258–265, Feb. 2000.
- [13] J. A. Ruiz-Cruz, M. A. El Sabbagh, and K. A. Zaki, "Canonical ridge waveguide filters in LTCC or metallic resonators," *IEEE Trans. Microw. Theory Tech.*, vol. 53, no. 1, pp. 174–182, Jan. 2005.
- [14] H.-T. Hsu, Z. Zhang, K. A. Zaki, and A. E. Atia, "Parameter extraction for symmetric coupled-resonator filters," *IEEE Trans. Microw. Theory Tech.*, vol. 50, no. 12, pp. 2971–2978, Dec. 2002.



Yunchi Zhang (S'04) received the B.S. and M.S. degrees in physics from Peking University, Beijing, China, in 1997 and 2000, respectively, the M.S. degree in electrical and computer engineering from North Carolina State University, Raleigh, in 2002, and is currently working toward the Ph.D. degree at the University of Maryland at College Park.

He is currently a Research Assistant with the Microwave Laboratory, Department of Electrical and Computer Engineering, University of Maryland at College Park. His current research interests include

analysis, modeling, and design of microwave and millimeter-wave devices and circuits.



Kawthar A. Zaki (SM'85–F'91) received the B.S. degree (with honors) from Ain Shams University, Cairo, Egypt, in 1962, and the M.S. and Ph.D. degrees from the University of California at Berkeley, in 1966 and 1969, respectively, all in electrical engineering.

From 1962 to 1964, she was a Lecturer with the Department of Electrical Engineering, Ain Shams University. From 1965 to 1969, she was a Research Assistant with the Electronics Research Laboratory, University of California at Berkeley. In 1970, she joined the Electrical Engineering Department, University of Maryland at College Park, where she is currently a Professor of electrical engineering. She has authored or coauthored over 200 publications. She holds five patents on filters and dielectric resonators. Her research interests are in the areas of electromagnetics, microwave circuits, simulation, optimization, and computer-aided design of advanced microwave and millimeter-wave systems and devices.

Prof. Zaki was the recipient of several academic honors and awards for teaching, research, and inventions.

Andrew J. Piloto received the B.S. degree in mechanical engineering and B.S. degree in solid-state physics from the University of Texas, Austin, in 1984 and 1985, respectively. From 1994 to 1996, he attended the Graduate School of The Johns Hopkins University, Baltimore, MD, under the graduate educational program of Westinghouse Electronics Systems.

He is currently a Member of the Technical Staff with the Product Technology Center, Kyocera America, San Diego, CA. He is currently involved in the development of next-generation transmit/receive (T/R) module and radar support electronics packaging for active phased-array radar systems. He was a Process Engineer with the Hybrid Microelectronics Laboratory, and a Design Engineer with the Advanced Missile Systems Department, Texas Instruments Incorporated. He participated in the design of ATF T/R modules for the F-22 and YF-23, as well as several classified programs. He was also with Northrop Grumman Electronic Systems (formerly Westinghouse Electronic Systems), where he was involved with the development of advanced T/R modules. While with Northrop Grumman Electronic Systems, he was granted 44 U.S. patents, two of which include both the JSF (F-35) T/R module and the stealthy ferrite used in the JSF circulator assembly. Upon leaving Northrop Grumman Electronic Systems, he co-founded the Design Integrated Circuits Division, Nurlogic, where he led opto-electronic (OE) integrated-circuit (IC)

development. Subsequently sold to Artisan Components, Nurlogic led the OE IC industry producing the first 72-channel parallel optical transceiver currently deployed in Cisco routers. He is currently involved with the development of highly integrated T/R modules and frequency converters for both space and terrestrial applications as both a contractor to the U.S. Government, as well as the original equipment manufacturers (OEMs).



Joseph Tallo received the B.S. degree in electrical engineering from the University of California at San Diego, La Jolla, in 2000.

He has been a Research and Design Engineer with Kyocera America, San Diego, CA. His research involves modeling and measurement of ceramic packages.